Probiotic Alleviate Fluoride-Induced Memory Impairment by Reconstructing Gut Microbiota in Mice

Jinge Xin
Sichuan Agricultural University
Hesong Wang
Southern Medical University Nanfang Hospital
Dong Zeng
Sichuan Agricultural University
Ning Sun
Sichuan Agricultural University
Lianxin Li
Sichuan Agricultural University
Ye Sun
Southern Medical University Zhujiang Hospital
Abdul Khalique
Sichuan Agricultural University
Yan Zeng
Sichuan Agricultural University
Kangcheng Pan
Sichuan Agricultural University
Bo Jing
Sichuan Agricultural University
Yang Bai
Southern Medical University Nanfang Hospital
XueQin Ni (xueqinni@foxmail.com)
Sichuan Agricultural University https://orcid.org/0000-0003-3632-654X

Research

Keywords: fluoride, Lactobacillus johnsonii BS15, memory dysfunction, gut–brain axis, hippocampus, gut microbiota

Posted Date: October 9th, 2020

DOI: https://doi.org/10.21203/rs.3.rs-87485/v1

Version of Record: A version of this preprint was published at Ecotoxicology and Environmental Safety on June 1st, 2021. See the published version at https://doi.org/10.1016/j.ecoenv.2021.112108.

Abstract

Background

Fluoride which is widespread in our environment and food due to geological origin and industrial pollution has been identified as developmental neurotoxicants. Gut-brain axis provide new sight to the brain-derived injury. We hypothesized that fluoride-induced memory impairment was associated with gut dysbiosis, which could be prevented by improving the gut microbiota.

Methods

Mice were given fluoridated drinking water (sodium fluoride, 100 mg/L) for 70 days and administered with PBS or a probiotic strain, Lactobacillus johnsonii BS15 for 28 days prior to and throughout a 70 day exposure to sodium fluoride.

Results

Results showed that fluoride reduces the exploration ratio in Novel object recognition (NOR) test and the spontaneous exploration during the T-maze test in mice following an hour water avoidance stress (WAS), which were significantly improved by the probiotic. 16S rRNA sequencing showed a significant seperation in ileal microbiota between the fluoride-treated mice and control mice. Lactobacillus was the mainly targeting bacteria and significantly reduced in fluoride-treated mice. BS15 reconstructed the fluoride-post microbiota and increased the relative abundance of Lactobacillus. D-lactate contant and diamine oxidase (DAO) activity, two biomarkers of the gut permeability were reduced in the serum of probiotic-inocluated mice. ZO-1, an intestinal tight junction protein, which was reduced by fluoride in mRNA and protein levels were increased by the probiotic treatment. Moreover, in the hippocampus which is essential to learning and memory, the probiotic increased the down-regulated mRNA levels of myelinassociated glycoprotein (MAG) level, Bcl-xl and decreaed up-regulated mRNA levels of Bad in fluoride-treated mice. The probiotic applied in this study also increased down-regulated mRNA and protein levels of brain-derived neurotrophic factor (BDNF) and cAMP response element-binding protein (CREB), and balanced the inflammatory cytokines in mRNA and protein levels in hippocampus of fluoride-treated mice.

Conclusions

These results suggested that there may be some correlations between the fluoride-induced memory dysfunction and alteration of gut microbiota, and reconstruction of gut microbiota is a potential method to prevent the memory dysfunction.

Background

Fluoride is a widespread environmental pollution, and ground water is the major source of exposure in which the fluoride concentration can be as high as 35 mg/L (Petrone, et al. 2013). Fluorosis induced by geological origin is a serious public health concern in 28 nations particularly in India and China (Rafique,

et al. 015). In India, 230 districts of 20 states are at risk of high level of fluoride in drinking water (Srivastava, et al. 2020). In China, almost all the provinces have reported fluorosis except for Shanghai. Moreover, social modernization results in fluoride pollution because of industrial production, the mechanical processing of food, and the use of fluorine-containing crop protection. Based on previous reports, fluoride concentration in canned meat and brick tea is under 1 to more than 8.6 mg/kg (Fein, et al. 2001) and 600–2800 mg/kg (Fung, et al. 1999), respectively. Fluoride accumulation in our body can damage both bone (Petrone, et al. 2013) and non-bone tissues (Yan, et al. 2019; Qian, et al. 2013), such as the liver, kidney, spleen, and brain. The neurotoxic effects of fluorine must not be ignored because such effects can affect brain health in rodents at levels below those that induce dental lesions (Grandjean, et al. 2019). To date, fluoride has been identified as developmental neurotoxicants (Grandjean, et al. 2014).

Recently, evidence on fluoride-induced brain damage is increasing and focused on learning and memory dysfunction. An epidemiological study from Hulunbuir, Inner Mongolia of China based on 331 children aged 7 to 14 from four schools with the same teaching quality demonstrated that fluoride exposure even in low levels had negative effects on children's memory (Ding, et al. 2011). Similar studies were also found in other countries (Green, et al. 2020; Bashash, et al. 2017). Moreover, Liu et al. (2010) found that a rat exposed to fluoride (50 mg NaF/L) for 6 months showed prolonged escape latency in the Morris water maze test. Animal experiments also demonstrated that fluoride exposure could cause microtubule lesions; thickened postsynaptic density; pathologic, indistinct, and short synaptic cleft; and myelin damage (Niu, et al. 2018). Furthermore, brain-derived neurotrophic factor (BDNF) and cAMP/Ca^{2+}-responsive element-binding protein (CREB), which have been identified to be involved in hippocampal plasticity and hippocampus-dependent memory based on considerable evidence, were decreased in mice exposed to fluoride (100 mg NaF/L) for 60 days (Niu, et al. 2018).

Recently, increasing evidence has demonstrated that the gut microbiota is associated with mood and memory disturbances, and improving the gut microbiota is a potential method to treat such diseases. For example, patients with colitis characterized by disordered gut microbiota have a high risk for anxiety (21%) and depression (15%) (Neuendorf, et al. 2016). Different colitis models represent the human behavioral phenotype. Zhao et al. (2020) found that the depression and anxiety-like behavior in dextran sulfate sodium-induced colitis model could be improved by lycopene through increasing the relative abundance of *Bifidobacterium* and *Lactobacillus*. Similarly, Jang et al. (2018) inoculated *Lactobacillus johnsonii* to 2,4,6-trinitrobenzenesulfonic acid-induced colitis model, which improved memory impairment by restoring the disturbed gut microbiota composition. Neuroactive metabolites and gut integrity are the main mechanisms underlying the communication between the gut and brain. Recently, Mao et al. (2020) observed increased levels of lactate in the fecal and brains of mice inoculated with *Lactobacillus*, and consequently, the mice had an improved memory. High levels of GABA are linked to novel object recognition and improved working memory and are consumed and produced by the gut microbiota, which influence circulating GABA levels (Strandwitz, et al. 2018). Damage of gut integrity can cause the bacteria and harmful metabolites to enter into the brain. Recently, Emery et al. (2017) found evidence for microbiological incursion into the brain. Zhan et al. (2016) found increased levels of *Escherichia coli* K99

and lipopolysaccharide (LPS) in Alzheimer's disease (AD) brain and suggested that Gram-negative bacteria-derived LPS induced AD neuropathology in an ischemia–hypoxia rat model. Collectively, these studies indicate a link between the gut microbiota and memory potential.

In addition, Luo et al. (2016) found that *Lactobacillus* spp. remarkably decreased and *E. coli* and *Enterococcus* spp. increased in fluoride-treated broiler. Therefore, we hypothesized that fluoride-associated memory impairment might be associated with gut microbiota changes. The present study aimed to determine the fluoride-exposed gut microbiome feature and assess whether adjusting the gut microbiota could alleviate the fluoride-induced memory dysfunction. Groups of mice were exposed to 100 ppm fluoride on the basis of (i) documented human exposures (The range of fluoride dose in adult is 0.84-27.1 mg per day, which convert to ppm is 0.19-6.02ppm [based on a 55 kg person drinking 4.5 L of water per day]; Supplementary Note 1 and Table S1), (ii) a dose equivalent equation adjusting for surface area differences between mice and humans (Coryell, et al. 2018) (Supplementary Note 1), (iii) the use of similar exposures in studies researching fluoride-associated brain lesion in mice (Table S2), and (iv) high dose for the potential damage in a shortened test period. We selected *L. johnsonii* BS15 (CCTTCC M2013663) as a potential strategy to regulate the gut microbiota. *Bifidobacterium* and *Lactobacillus* strains are commonly used to improve the gut microbiota. *L.johnsonii* BS15 (CCTTCC M2013663), which has been screened and separated by our team, showed a steady effect on adjusting the gut environment and lowering the intestinal permeability of mice with high-fat diet, thereby preventing non-alcoholic fatty liver disease (Xin, et al. 2014). We recently found that *L. johnsonii* BS15 improved memory dysfunction in mice induced by a 7 day water-avoidance stress (WAS) by enhancing the gut integrity, which could be a potential "psychobiotic" (Wang, et al. 2020). We used 16S rRNA gene sequencing to detect the feature of the gut microbiota in fluoride-infected mice and BS15-treated mice. We assessed the difference in memory ability between untreated and treated individuals by T-maze test and novel object recognition (NOR) test under psychological stress. Given the importance of the hippocampus on memory function, hippocampal inflammation and memory-associated protein were detected in this study. This study may provide new insight to the fluoride-induced memory impairment and novel method to prevent these impairment.

Materials And Methods

Culture and Treatment with BS15

L. johnsonii BS15 was grown under anaerobic condition in de Man–Rogosa–Sharpe broth (Qingdao Rishui Bio-technologies Co., Ltd., Qingdao, China) at 37 °C for 24 h. The quantity of bacterial cells was assessed by heterotrophic plate counts. *L. johnsonii* BS15 cells were then centrifuged (10,000×g, 10 min at 4 °C), washed three times by phosphate-buffered saline (PBS), and re-suspended in PBS (pH 7.0) at a density of 1×10^9 cfu cells/mL (daily consumption dose: 0.2 mL/mice).

Water avoidance stress (WAS)

WAS, a well-established model of psychological stress in mice, was used in our study as a psychological stressor. Mice were exposed to WAS, as Gareau et al. (2011) described with minor modifications. In brief, mice were placed on a small platform surrounded by room-temperature water (1 cm below the platform) in the middle of the home cage for 1 h. All the WAS and behavioral tests were carried out at 7:00 am–11:30 am.

Behavioural tests

NOR test: The NOR test was used to assess the ability of rodents to recognize a novel object in the environment. It is a widely used method for the detection of working memory alterations based on nature propensity for novel objects displayed by rodents. The task procedure included three phases (Antunes and Biala, 2012): habituation, familiarization, and test phase. In brief, in the habituation phase, each mouse was placed into the empty open-field arena (l×b×h=40 cm×40 cm×45 cm) for 1 h for habituation. The mouse was then removed from the arena and placed in its home cage. During the familiarization phase, one mouse, following 1 hour WAS, was placed in the arena containing two different objects (#A+#B) for 5 min. These two objects were placed in opposite corners of the cage. Then, the mouse was removed from the arena and returned to its cage for a 20 min rest. During the test phase, the mouse was returned to the arena and confronted with object B and a novel object (object #C, distinguishable from object #A). Exploration ratio (F#C/(F#C + F#B) × 100, F#C = frequency of exploring the object #C, F#B = frequency of exploring the object #B), which was used to assess the memory, was calculated.

The tendency of mice to explore novelty indicated that the presentation of the familiar object existed in their memory. The objects used included a green bottle cap (#A), orange bottle cap (#B), and a small smooth stone (#C).

T-Maze test: Enclosed T-maze, an apparatus with 10 cm-wide floor and 20 cm-high walls in the form of a “T” placed horizontally, was used. The stem of the two goal arms and a start arm was all 30 cm long. A central partition was placed in the middle of two goal arms extending into the start arm (7 cm). Every arm had a guillotine door. The apparatus and operating steps were consistent with Deacon and Rawlins(2006). First, the central partition was placed in the T-maze with all the doors open. Then, mouse, directly from its home cage or flowing exposure to WAS, was placed in the start area and allowed to select the left or right arm. The mouse was kept in the chosen arm by quietly sliding the door down. After 30 s, the mouse and central partition were removed, and the mouse was returned to its holding cage. After a retention interval of 1 min, the mouse was placed in the start area for a second trail with all the doors open. Each mouse was given 10 trials over 5 days and allowed to explore the maze before sated. If the mouse selected the other goal arm in consecutive trials, then this trial was marked as “correct.” Each exploration should take no more than 2 min.

Establishment of an animal model and study design

Male ICR mice (3 weeks old, Chengdu Dashuo Biological Institute, Chengdu, China) were given 1 week to adapt to the new environment. After the adaptation period, mice were randomly divided into three groups

and administered with either PBS (control group, F group) or *L. johnsonii* BS15 (prob group; 0.2 mL/day) for 28 days prior to and throughout a 70 day exposure to sodium fluoride. Mice were provided fluoridated drinking water (concentration: 100 mg NaF/L) from 28 days to 98 days, except for the control group. Mice were housed in a constant-temperature (20 °C–22 °C) room with a 12 h light/dark cycle (lights on from 06:00 to 18:00) and given free access to water and normal chow diet (Chengdu Dashuo Biological Institute). Each cage housed six mice.

On day 98 of the experiment, subsets of mouse in each group were sacrificed by cervical dislocation for sampling following exposure to 1 h WAS. Another 10 mice of each group were used for behavioral testing after exposure to 1 h WAS. Subsets of mouse in each group without acute stress were sacrificed for sampling baseline gut microbiota.

Blood was sampled from the mice orbit, and serum was separated by incubation at 4 °C for 30 min, followed by centrifugation at 2,000×g for 20 min, and stored at −30 °C. The left hippocampus and partial ileal tissue were removed and washed with ice-cold sterilized saline without RNA enzyme (RNase) and then immediately frozen in liquid nitrogen for gene expression analysis. The right hippocampus and partial ileal tissue were obtained and stored at −80 °C for further biochemical detection. Luminal sample was collected from the ileum and stored at −80 °C for analysis of lumen-associated microbiome based on 16S rRNA gene sequencing. The ileal content was collected and stored at −80 °C for 16S rRNA gene sequencing.

Biochemical evaluation

The ileal tissue and right hippocampus were ground (pH 7.4) into 10% or 5% homogenate with PBS, respectively, and then centrifuged (12,000×g for 5 min at 4 °C). The obtained liquid supernatant was used for biochemical detection. The D-lactate and diamine oxidase (DAO) activity, contents of corticosterone (CORT) in the serum, the inflammatory cytokines in the liquid supernatant of the ileum and hippocampal homogenate, and apoptosis-regulated proteins in the liquid supernatant of hippocampal homogenate were measured by the commercial enzyme-linked immunosorbent assay (ELISA) kit for mice according to the manufacturer's instructions. The inflammatory cytokines included tumor necrosis factor-alpha (TNF-α), interleukin-1β (IL-1β), IL-6, interferon-gamma (IFN-γ), and IL-10 (only detects ileal tissue). All the commercial ELISA reagent kits were obtained from Enzyme-linked Biotechnology Company (Shanghai Enzyme-linked Biotechnology Co., Ltd., China).

Real-time quantitative polymerase chain reaction (qPCR) analysis of gene expression

Total hippocampal RNA and ileal RNA were isolated using E.Z.N.A.® Total RNA Kit (OMEGA Bio-Tek) according to the manufacturer's instructions. Isolated RNA was assessed from the ratio of absorbance at 260 and 280 nm and agarose gel electrophoresis for quantitative and qualitative analyses. The isolated RNA was transcribed into first-strand complementary DNA with PrimeScript RT reagent kit with gDNA Eraser (Thermo Scientific, Waltham, Massachusetts, USA) according to the manufacturer's instructions. qPCR was performed with SYBR green and primers (details previously published) (Xin, et al. 2014). The

PCR conditions were as follows: 1 cycle at 95 °C for 5 min, followed by 40 cycles at 95 °C (10 s) and optimum temperature (30 s), and then a final melting curve analysis to monitor the purity of the PCR product. The optimum temperature of each gene was shown in Table S3. β-Actin was used as reference genes to normalize the relative mRNA expression levels of target genes with values presented as $2^{-\Delta\Delta Cq}$. Primer sequences and optimum annealing temperatures were shown in Table S3. The relative expression levels of neurogenesis-related factors (BDNF, CREB, SCF, and NCAM), molecular myelin structure (MOG, PLP, MBP, and MAG), apoptosis-related proteins (Bax, Bad, Bcl-2, Bcl-xl, casepase9, and casepase3), cytokines (IFN-γ, TNF-α, IL-1β, IL-6, and IL-10) in the hippocampus, and tight junction (TJ) proteins (ZO-1, claudin-1, and occludin) in ileal tissue were detected.

Immunohistochemistry

A subset of mice in each group was sacrificed, and their brain was removed, fixed in 4% paraformaldehyde solution, and stored in 4 °C for immunohistochemical assay. The brain tissues were embedded by paraffin and cut by a microtome. Slices were submerged in citrate antigen retrieval solution and heated at medium heat until boiling using a microwave oven (model: P70D20TL-P4; Galanz, Guangdong, China). The temperature was ceased, and the tissues were kept warm for 8 min. Then, the tissues were heated at medium–low heat for 7 min. After free cooling, the slices were placed into PBS (pH 7.4) and shaken for 5 min for decoloration, which was repeated three times. Afterward, the sections were incubated in 3% oxydol for 25 min at room temperature and away from the light to block endogenous peroxidase. The slices were washed three times in PBS by shaking for 5 min, then sealed for 30 min by 3% bull serum albumin, and incubated with monoclonal rabbit anti-Occludin, anti-Claudin-1, or anti-ZO-1 (1:200) antibodies at 4 °C overnight. Species-specific biotinylated anti-rabbit immunoglobulin (horseradish peroxidase labeled) was used for immuno-detection. Following the second antibody incubation, the 3,3'-diaminobenzidine staining kit was used to complete the reaction according to the manufacturer's instructions. Hematoxylin staining was performed to re-stain the nucleus.

16S rRNA gene sequencing

Bacterial genomic DNA was extracted using the E.Z.N.A.TM stool DNA isolation kit (Omega Bio-Tek, Doraville, CA). The final elution volume was 100 μL, and the integrity, purity, fragment size, and concentration were determined by electrophoresis with 1% agarose gel. The 16S V3-V4 was amplified by PCR using the primer 515F/806R of the 16SrRNA gene. Then, the purified PCR products were formed into a library with Ion Plus Fragment Library Kit 48 rxns (Thermofisher, USA) and sequenced in the Ion S5™XL platform (Thermofisher, USA) using the single-end sequencing. The primer contained adapter sequences and single-end barcodes, allowing pooling and direct sequencing of PCR products. Cutadapt (V1.9.1, http://cutadapt.readthedocs.io/en/stable/) was applied to the resulting high-quality 16SrRNA gene reads. The 16S rRNA gene read pairs were demultiplexed on the basis of the unique molecular barcodes, and reads were merged using VSEARCH (Rognes, et al. 2016). Sequences were clustered into operational taxonomic units (OTUs) at a similarity cutoff value of 97%. Then, OTU representative sequences were produced using the Uparse v7.0.1001. Species annotation analysis was performed on the OTU

representative sequences through the SILVA Database. Homogenized data of each sample were constructed using the sample with the least amount of data as the standard. This sample was used for downstream analyses of alpha-diversity, beta-diversity, phylogenetic trends, and functional prediction.

Statistical analysis

The 16S rRNA sequencing data were analyzed by T-test, Wilcoxon rank-sum test, or Tukey test to detect significant differences among the different groups. All other results were reported by mean ± standard deviation. Groups were compared using Student t-test and one-way analysis of variance (ANOVA) with Duncan's multiple range test for significant difference test. Differences of $p<0.05$ were considered as statistically significant.

Results

As shown in Figs. 1A and 1B, the spontaneous exploration in the T-maze test and the exploration ratio in the NOR test were significantly reduced in the F group compared with the control and prob groups. No significant difference was observed in the abovementioned indexes between the control and prob groups. Fig. 1C shows that the F group exhibited a remarkably higher serum CORT level than the other two groups, but no significant difference was found between the other two groups.

Figs. 2A and 2B show a sharp decrease in mRNA expression levels of BDNF and CREB in the F group compared with the other two groups. The mRNA level of BDNF in the control group was higher than that in the prob group (Fig. 2A). No difference was observed in the CREB mRNA level between the control and prob groups (Fig. 2B). Moreover, no significant difference was found among the three groups (Fig. 2C). Compared with the control group, the SCF mRNA level was remarkably reduced in the F group and slightly decreased in the prob group (Fig. 2D). By contrast, the prob group presented a slightly higher SCF mRNA level than the F group (Fig. 2D). As shown in Figs. 2E–2J, the protein expression levels of BDNF and CREB were significantly reduced in the F group compared with that in the other two groups.

As shown in Figs. 3A and 3D, TNF-α and IFN-γ protein levels were significantly increased in the F group compared with that in the control and prob groups. However, the mRNA level of the abovementioned indexes in the F group was significantly higher than the control group. This difference was slight compared with the prob group. Similarly, the mRNA level of the abovementioned indexes in the prob group was slightly higher than that in the control group. However, the prob group presented significantly higher TNF-α and IFN-γ protein levels than the control group. No significant difference in IL-1β among the three groups was found in the mRNA and protein levels (Fig. 3B). As shown in Fig. 3C, the F and prob groups showed a lower IL-6 than the control group both in the mRNA and protein levels. Compared with the prob group, the significant increase of IL-6 in the F group was observed in the protein level but not in the mRNA level.

Figs. 4A and 4B show that the mRNA expression levels of PLP and MOG in the F and prob groups were sharply decreased compared with that in the control group. The PLP in the prob group was slightly higher

than that in the F group. No significant difference in the MOG was observed between the F and prob groups. No changes in the MBP mRNA expression level were observed among the three groups (Fig. 4C). As shown in Fig. 4D, the F group presented a significantly lower MAG mRNA level than the other two groups. Compared with the control group, MAG was remarkably reduced in the prob group (Fig. 4D).

No significant difference in the Bcl-2 mRNA level was found among the three groups, whereas the prob group showed the highest among the three groups (Fig. 5A). In Fig. 5B, the F group presented a lower Bcl-xl mRNA level than the other two groups, but no difference was observed in the other two groups. As shown in Fig. 5C, the Bax mRNA level in the F group was slightly increased compared with that in the other two groups, but no significant difference was observed among the three groups. Fig. 5D shows a remarkably increased Bad mRNA level in the F group compared with the other two groups, whereas no difference was observed in the other two groups. As shown in Figs. 5E and 5F, no significant difference in the casepase3 and casepase9 mRNA level was observed among the three groups, but casepase3 in the control group and casepase9 in the F group were the lowest and highest, respectively, among the three groups.

The gut microbiota with or without stress were observed in each group to determine the influence of fluoride and acute stress on the gut microbiota. Through 16s rRNA gene sequencing, we did not find significant alterations in the gut microbiota of mice exposed to WAS versus non-stressed animals (Fig. S1, supplementary materials). Thus, the data with or without WAS were combined in each group.

As shown in Figs. 6A and 6B, principal coordinate analysis based on unweighted UniFrac distances and principal component analysis showed a clear separation between the ileal microbiota of mice in the F group and those in the other groups, whereas no significant separation was observed between the other two groups. Moreover, the observed species (Fig. 6C) and Shannon index (Fig. 6D) in the ileal lumen microbiome of mice in the F group were significantly increased compared with that in the control group, whereas significant increases were not observed in the prob group. The ileal microbial communities among the three groups were dominated by *Firmicutes* in the phylum level (Fig. 6E). As shown in Fig. 3F, relative abundance of *Firmicutes* in the F group was significantly reduced compared with that in the control and prob groups. On the contrary, the relative abundances of *Actinobacteria* (Fig. 6G), *Bacteroidetes* (Fig. 6H), and *Cyanobacteria* (Fig. 6I) increased markedly in the F group compared with the control and prob groups. The alteration of these common phyla induced by fluoride was significantly inhibited by *L. johnsonii* BS15. At the genus level (Fig. 6J), *Lactobacillus* was the important bacterium in the control, F, and prob groups, and the relative abundance of the nine main genera found in the three groups was different. As shown in Fig. 6K–S, the F group presented a sharply reduced relative abundance of *Lactobacillus* and *Candidatus_Arthromitus* and a significantly increased relative abundance of *Streptococcus*, *Romboutsia*, *Allobaculum*, *unidentified_Clostridiales*, *Dubosiella*, *Bifidobacterium*, and *unidentified_Lachnospiraceae* compared with the control group. However, *L. johnsonii* BS15 suppressed these alterations except for *Streptococcus*, *unidentified_Clostridiales*, *Bifidobacterium*, and *Candidatus_Arthromitus*. Compared with the control group, more genera bloomed or diminished in the ileal lumen of the F group than those in the prob group (Fig. 6T).

As shown in Figs. 7A and 7D, the F group showed a sharp increase in the mRNA and protein levels of TNF-α and IFN-γ compared with the other two groups, but no significant difference was observed between the other two groups except for the TNF-α mRNA level. Fig. 7B shows that the control group presented a lower IL-1β mRNA and protein levels than the other two groups, but no marked difference was found between the other two groups. No difference was observed in the IL-6 mRNA and protein levels among the three groups (Fig. 7C). Fig. 7E shows a sharp decrease in the IL-10 mRNA and protein levels in the F group than the other two groups, but no difference was found between the other two groups.

As shown in Fig. 8A, the F group shows a markedly lower ZO-1 mRNA level than the other two groups, but significant difference was not observed in the other two groups. Compared with the control group, the mRNA expression levels of claudin-1 and occludin were sharply decreased in the F and prob groups. No significant difference was observed in claudin-1 mRNA level between the control and prob groups. The occludin mRNA level in the prob group was slightly higher than that in the F group. The protein expressions of TJs were also detected by immunohistochemistry, and the results showed the same trend (Fig. 8C).

As shown in Fig. 8B, compared with the control group, the serum DAO content was significantly and slightly increased in the F and prob groups, respectively. The control group showed a remarkably lower serum D-lactate activity than the other two groups. By contrast, the D-lactate activity in the F group was significantly higher than that in the prob group.

Discussion

The results of this study provided strong evidence that reconstructing the gut microbiota could protect the brain from fluoride-induced damage and dysfunction under acute stress. Several lines of evidence supported the conclusion. First, fluoridated drinking water altered the gut microbiota structure and resulted in a reduced hippocampal BDNF and poor performance in memory-associated behavioral tests under psychological stress. Second, these alterations were reversible upon reconstruction of the microbiota by gavage with *L. johnsonii* BS15.

A 70 day exposure to sodium fluoride combined with 1 h exposure to WAS lowered memory potential in this experiment, indicated by the low spontaneous exploration in T-maze test and low exploration ratio in NOR test. In our previous study, different exploration ratios in NOR test were not observed between the F and control groups in the absence of WAS (data not shown). WAS is a commonly used psychological stress. Studies found that an hour of WAS exposure could not induced behavioral changes in the T-maze and NOR tests but could cause compounding effect on behavior when combined with other harmful materials (e.g., endotoxin exposure and bacterial infection) by enhancing the HPA axis responsiveness (Gareau, et al. 2011; Walker, et al. 2008). Thus, an hour of WAS exposure was added to make the potential memory impairment more evident in this experiment. Consequently, fluoride exposure resulted in HPA hyper-responsiveness to stress, indicated by abnormal elevated serum CORT in fluoride-treated mice compared with the control mice. This result was consistent with predecessors' research (Gareau, et al.

2011). Apart from the behavioral phenotypes, memory-associated gene expressions were assessed in the RNA and/or protein levels. Neuronal plasticity is the basic of learning and memory and occurs by neurogenesis, synaptic-dependent activity, cellular apoptosis, and reorganization of neuronal networks. The hippocampus, a highly plastic region, is critical for learning and memory. BDNF is one of the important modulators of neuroplasticity because of its multiple effects, such as increasing hippocampal neurogenesis, dendritic branching, cell proliferation, and promoting hippocampal long-term potentiation (Pang, et al. 2004; Cassilhas, et al. 2016). Blocking the hippocampal BDNF expression caused an impairment of spatial and reference memory (Mizuno, et al. 2000). CREB, the transcriptional regulator of BDNF, has been considered as the central to AD pathology by similar genomic network analysis (Jeong, et al. 2001). In addition, many studies using genetically modified mice revealed that a growing number of genes, such as CREB, BDNF, NCAM, and SCF, were involved in the regulation of neurogenesis. In the present study, fluoride showed adverse effects on neuroplasticity as indicated by the remarkable decrease in the expressions of BDNF, CREB, and SCF on the mRNA and/or protein levels, which was consistent with the observations of Niu et al. (2018). Buffington et al. (2016) reported that the behavioral deficits and disordered gut microbiota in maternal high-fat diet offspring could be recovered by co-housing the offspring of mothers on a regular diet. Kumar et al. (2017) suggested that *L. johnsonii* could increase the concentrations of acetate and butyrate in feces. Butyrate, a short-chain fatty acid, could decrease BDNF methylation and consequently cause an overexpression of BDNF by decreasing 10 to 11 translocation methylcytosine dioxygenase 1, which was the enzyme responsible for catalyzing the conversion of DNA methylation to hydroxymethylation (Wei, et al. 2014). Moreover, Luo et al. (2016) found that *Lactobacillus* spp. was significantly reduced in fluoride-treated broiler. Thus, *L. johnsonii* BS15 was supplemented to fluoride-treated mice to investigate whether *L. johnsonii* BS15 could reconstruct the gut microbiota and alleviate memory impairment. Memory was assessed using the same T-maze and NOR tests in the *L. johnsonii* BS15-inoculated mice and compared with that of control and F-treated mice. Based on our data, the *L. johnsonii* BS15-inoculated mice showed a significant improvement in memory compared with fluoride-treated mice. Furthermore, the negative effects of fluoride treatment on the HPA response, BDNF, and CREB have been reversed by *L. johnsonii* BS15. Fluoride treatment showed significantly adverse effects on the SCF expressions, which were not improved by administering *L. johnsonii* BS15. Thus, *L. johnsonii* BS15 prevented memory impairment in fluoride-infected mice, mediated the upregulations in BDNF and CREB, and attenuated the HPA response to an acute psychological stress to a certain extent.

Chronic neuroinflammation attracts public attention for its role in mental health and diseases. However, considerable evidence proved that fluoride accumulation could activate microglia, a resident macrophage in the CNS, and lead to the production of proinflammatory cytokines. Prior studies have noted the importance of aberrant intestinal microbiota, altered intestinal immune response, and impaired intestinal barrier on the neuroinflammation (Salehipour, et al. 2017). A possible mechanism underlying *L. johnsonii* BS15, which protected mice from fluoride-induced memory impairment, could be the inhibition of neuroinflammation. We quantified inflammatory cytokines in both mRNA and protein levels in the hippocampus to test this possibility. Inconsistent with previous studies (Guo, et al. 2017), we found that fluoride increased the TNF-α mRNA level in the hippocampus. In addition, hippocampal IFN-γ was

increased in fluoride-infected mice under acute stress. Nevertheless, the effect of chronic fluorosis on the level of IL-6 was controversial. Yan et al. (2016) reported that the protein expression level of IL-6 was increased in microglial cells of rats exposed to fluoride. Moreover, evidence has shown that fluorosis inhibited the activity of immune cells resulting in the reduction and secretion of IL-6 (Guo, et al. 2017), which was consistent with our results that excessive fluoride intake could reduce IL-6. Early studies showed that high level of TNF-α could reduce synaptic density in the hippocampus (Salucci, eta al. 2014). Considerable evidence has suggested that IL-6 has a modulatory effect on TNFα-induced hippocampal injury (Harry, et al. 2003), and high level of TNF-α and low level of IL-6 might mediate the altered hippocampal volume and verbal memory difficulties (Kesler, et al. 2013). Supplement with *L. johnsonii* BS15 ameliorated neuroinflammation in the stressed and fluoride-infected mice by reducing the hippocampal TNF-α and IFN-γ and increasing IL-10. This finding was consistent with that of Salehipour et al., who reported that probiotic was a potential therapy to attenuate chronic CNS inflammation (Salehipour, et al. 2017). Sun et al. also demonstrated that reversing gut microbial dysbiosis could reduce the activation of the TLR4/TNF-a signaling pathway in microglia and astrocytes of Parkinson's disease (PD) mice and recover motor dysfunction of PD mice (Sun, et al. 2018). On the basis of the abovementioned results, we could hypothesize that the reduced neuroinflammation in BS15-inoculated mice was associated with the alleviated memory impairment.

We observed the mRNA expression of myelin-associated protein to assess the effect of *L. johnsonii* BS15 on hippocampal impairment induced by fluoride. Previous studies have demonstrated that fluoride could induce demyelination (Niu, et al. 2018). Notably, myelin sheath constituted by MOG, PLP, MBP, and MAG was important for axonal protection and interneuronal communication (Nguyen, et al. 2009). In accordance with the previous studies, the present results showed that fluoride significantly reduced the PLP and MAG in the hippocampus (Niu, et al. 2018). In addition, in this study, hippocampal PLP was significantly reduced, which might be due to the longer time of fluoride exposure or the acute stress exposure. MAG located in the innermost lamellae of myelin sheaths, as an inhibitor of mature axonal regeneration, could also promote stability and survival of myelinated axons (Nguyen, et al. 2009). A local downregulation of MAG is the critical signal for CNS injury (Nguyen, et al. 2009). Treatment with *L. johnsonii* BS15 effectively inhibited the reduction of MAG in fluoride-infected and stressed mice. Moreover, *L. johnsonii* BS15 upregulated the mRNA expression of Bcl-xl (anti-apoptotic) and downregulated the mRNA expression of Bad (pro-apoptotic) in the hippocampus of fluoride-infected and stressed mice, indicating that hippocampal apoptosis was linked to fluoride-induced memory impairment, whereas *L. johnsonii* BS15 improved hippocampal apoptosis.

The gut microbiota is a key modulator of the bidirectional signaling pathways between the gut and brain. We conducted 16S rRNA gene sequencing on the ileal contents of mice to identify whether the reconstruction of gut microbiota was a potential mechanism underlying the hypothesis that BS15 protected mice from memory impairment induced by fluoride. An hour of WAS exposure did not significantly change the gut microbiota structure (Fig. S1 and Table S4). We substantiated the composition differences of the gut microbiota in fluoride-treated mice through Adonis testing (Table S5) and unweighted analyses of UniFrac distances, and the administration of *L. johnsonii* BS15 reversed

those differences. *Firmicutes*, which accounted for up to 90% of the total sequences, was the dominant phylum in each group. Disordered gut microbiota in fluoride-exposed mice was primarily manifested by the relative abundance decrease of *Firmicutes* in the phylum level and *Lactobacillus* in the genus level. *Lactobacillus* is an important genus in *Firmicutes*. The relative abundance of *Lactobacillus* in the control, F, and prob groups was 87.7%, 38.1%, and 72.7%, respectively. The reduction of *Lactobacillus* induced by fluoride was consistent with the results of Luo et al. (2016) Spearman correlation analysis in the genus level of the control group showed that *Lactobacillus* was negatively associated with most of the bacteria (66.7%; Fig. S2A). In addition to the reduction of *Lactobacillus*, the abovementioned negative association between *Lactobacillus* and most bacteria was weakened and shifted to positive association in the F group (Fig. S2B), indicating that the inhibiting effect of *Lactobacillus* on other bacteria was weakened, which explained the increases in community diversity (Shannon index) and richness indices (number of observed features) in fluoride-infected mice. The administration of *L. johnsonii* BS15 reversed these changes (Fig. S2C). This finding was in accordance with that of previous studies, which have suggested that *Lactobacillus* could suppress the growth of other bacteria, particularly harmful bacteria, because of its enzymatic, fibrinolytic, and broad-spectrum antimicrobial activity (Eom, et al. 2015). New evidence by 16S rRNA gene sequencing of the gut microbial community in the genetically defined collaborative cross mouse cohort with different memory potentials showed that higher relative abundances of *Lactobacillus* indicated higher memory potential (Mao, et al. 2020). This result was in accordance with that of Gareau et al., who showed that BDNF could reduce the risk of disorder and increase the stability of the gut microbiota (Gareau, et al. 2011). The alteration of microbiota composition indicated that the reconstruction of the gut microbiota might be an important potential mechanism underlying the improvement of memory in BS15-inoculated mice.

On the basis of recent reports, which associated bacteria and their products with memory in human (Emery, et al. 2017; Zhan, et al. 2016) (e.g., *E coli* K99, LPS), we focused on understanding the alterations of gut inflammation and intestinal integrity underlying the improvement of memory in gut microbiota-reconstructed mice. We observed increased pro-inflammatory cytokines (TNF-α, IL-1β, and IFN-γ) and decreased anti-inflammatory cytokine (IL-10) and TJ proteins (ZO-1, claudin-1, and occludin) in the mRNA and/or protein levels in the ileum of the F group, indicating an enhanced gut inflammation and damaged intestinal epithelial integrity. The increased serum DAO content and D-lactate activity in the F group also indicated that fluoride increased gut permeability. Serum DAO activity and D-lactate content, indicators of mucosal integrity, would be increased when the intestinal mucosal integrity was destroyed (Luk, et al. 1980; Ewaschuk, et al. 2005). Gut microbiota reconstruction improved gut inflammation and gut permeability. These findings were consistent with the previous findings that specific probiotic administration could improve gut inflammation and intestinal mucosa integrity (Mujagic, et al. 2017). Damaged intestinal mucosal integrity and some pro-inflammatory factors not only caused peripheral immune activation but also crossed the blood–brain barrier to aggravate neuroinflammation in the CNS under pathological conditions. Ait-Belgnaoui et al. also found that probiotic treatment could prevent leaky gut, thereby attenuating HPA response to an acute psychological stress in rats (Ait-Belgnaoui, et al. 2012). Hence, these results indicated that gut inflammation and intestinal mucosa integrity might be involved in

the pathogenesis of neurotoxic effects of fluoride and might be the primary reason that reversed gut microbiota improved memory deficit in fluoride-infected mice under acute stress.

Conclusion

This study showed that fluoride-exposed and stressed mice displayed impaired memory, damaged myelin, and a hyperactive HPA axis, coupled with a disordered gut microbiota structure particularly reduced relative abundance of *Lactobacillus*. Reconstruction of the gut microbiota by inoculating *L. johnsonii* BS15 could recover gut physiology, reverse memory deficit, alleviate myelin damage, and reduce the hyperactivity of the HPA axis. Collectively, our findings first indicated an importanat role of gut dysbiosis in improving memory impairment in fluoride-infected and stressed mice. Adjustment of the gut microbiota might be a potential treatment strategy to prevent food-borne memory damage.

Abbreviations

CNS, central nervous system; HPA, hypothalamic-pituitary-adrenal; CORT, corticosterone; NOR, object recognize; WAS, water avoidance stress; PBS, phosphate buffered saline; ELISA, enzyme-linked immunosorbent assay; OTUs, operational taxonomic units; BDNF, brain-derived neurotrophic factor; CREB, cAMP/Ca2+ responsive element-binding protein; SCF, stem cell factor; NCAM, neuronal cell adhesion molecule; MOG, myelin oligodendrocyte glycoprotein; PLP, proteolipid protein; MBP, myelin basic protein; MAG, myelin-associated glycoprotein; Bcl-2, B-cell lymphoma-2; Bcl-xl, B-cell lymphoma-extra large; Bax, Bcl2-associated X protein; Bad, Bcl-xL/Bcl-2 asociated death promoter; TNF-α, tumor necrosis factor-α; IL-β, interleukin-β; IL-6, interleukin-6; IFN-γ, interferon-γ; IL-10, interleukin-10; ZO-1, zonula occludens protein 1; DAO, diamine oxidase.

Declarations

Availability of data and materials

All data generated or analysed during this study are included in this published article [and its Additional file 9].

16S rRNA sequencing reads have uploaded to NCBI. The accession code of 16S rRNA sequencing reads in the National Center for Biotechnology Information (NCBI) BioProject database : PRJNA660154.

Ethics approval and consent to participate

All animal experiments were performed according to the guidelines for the care and use of laboratory animals approved by the Institutional Animal Care and Use Committee of Sichuan Agricultural University (approval number: SYXKchuan2019-187).

Consent for publication

'Not applicable' for that section

Competing interests

The authors declare that they have no competing interests

Funding

The present study was supported by National Natural Science Foundation of China (31970503) and Sichuan Science and Technology Program (2019YFH0060).

Authors' contributions

JX, HW, DZ, YB, and XN designed the experiment, such as Performing literature reviews, selecting search engines and search terms, and defining inclusion/exclusion criteria qualifies. JX, NS, LL, and AK performed the animal experiments and sample collection, and drafted the manuscript. YS, YZ, and KP helped to draft the manuscript. BJ and XN supervised the study.

Acknowledgements

The authors gratefully acknowledge the help from Ms. Peng Xueji and Mr. Zhang Shuai for all the hard working during the behavioral tests. Also, we really appreciate the supports provided by all other undergraduates during the animal feeding and sampling.

Authors' email addresses

JX: xinjinge@foxmail.com; HW: 236432291@qq.com; DZ: zend@sicau.edu.cn, NS: sunning132@foxmail.com; LL: 906800936@qq.com; YS: 1323312855@qq.com; AK: abdulkhalique36@gmail.com; YZ: yanzeng@sicau.edu.cn; KP: Pankangcheng71@126.com; BJ: 272682894@qq.com; YB: 13925001665@163.com; XN: xueqinni@foxmail.com.

References

Ait-Belgnaoui, A.; Durand, H.; Cartier, C.; Chaumaz, G.; Eutamene, H.; Ferrier, L.; Houdeau, E.; Fioramonti, J.; Bueno, L.; Theodorou, V. Prevention of gut leakiness by a probiotic treatment leads to attenuated HPA response to an acute psychological stress in rats. Psychoneuroendocrinology. 2012, 37, 1885-95.

Antunes, M.; Biala, G. The novel object recognition memory: neurobiology, test procedure, and its modifications. Cogn Process. 2012, 13, 93-110.

Bashash, M.; Thomas, D.; Hu H.; Martinez-Mier, E. A.; Sanchez, B. N.; Basu, N.; Peterson, K. E.; Ettinger, A. S.; Wright, R.; Zhang, Z.; Liu, Y.; Schnaas, L.; Mercado-García, A.; Téllez-Rojo, M. M.; Hernández-Avila, M. Prenatal fluoride exposure and cognitive outcomes in children at 4 and 6-12 years of age in Mexico. Environ Health Perspect. 2017, 125, 097017.

Buffington, S. A.; Prisco, G. V.; Auchtung, T. A.; Ajami, N. J.; Petrosino J. F.; Costa-Mattioli M. Microbial reconstitution reverses maternal diet-induced social and synaptic deficits in offspring. Cell. 2016, 165, 1762-1775.

Cassilhas, R. C.; Tufik, S.; Mello, M. T. Physical exercise, neuroplasticity, spatial learning and memory. Cell Mol Life Sci. 2016, 73, 975-83.

Coryell, M.; McAlpine, M.; Pinkham, N. V.; McDermott, T. R.; Walk, S. T. The gut microbiome is required for full protection against acute arsenic toxicity in mouse models. Nature communications. 2018, 9.

Deacon, R. M. J.; Rawlins, J. N. P. T-maze alternation in the rodent. Nat Protoc. 2006, 1, 7-12.

Ding, Y.; Gao, Y.; Sun, H.; Han, H.; Wang, W.; Ji, X.; Liu, X.; Sun, D. The relationships between low levels of urine fluoride on children's intelligence, dental fluorosis in endemic fluorosis areas in Hulunbuir, Inner Mongolia, China. J Hazard Mater. 2011, 186, 1942-6.

Emery, D. C.; Shoemark, D. K.; Batstone, T. E.; Waterfall, C. M.; Coghill, J. A., Cerajewska T. L.; Davies, M.; West, N. X.; Allen, S. J. 16S rRNA next generation sequencing analysis shows bacteria in Alzheimer's post-mortem brain. Front Aging Neurosci. 2017, 9, 195.

Eom, J. S.; Song, J.; Choi, H. S. Protective Effects of a novel probiotic strain of *Lactobacillus plantarum* JSA22 from traditional fermented soybean food against infection by salmonella enterica serovar typhimurium. J Microbiol Biotechnol. 2015, 25, 479-91.

Ewaschuk, J. B.; Naylor, J. M.; Zello, G. A. D-lactate in human and ruminant metabolism. J Nutr. 2005, 135, 1619-25.

Fein, N.J.; Cerklewski, F. L. Fluoride content of foods made with mechanically separated chicken. J Agr Food Chem. 2001, 49, 4284-4286.

Fung, K. F.; Zhang, Z. Q.; Wong, J. W. C.; Wong, M. H. Fluoride contents in tea and soil from tea plantations and the release of fluoride into tea liquor during infusion. Environ Pollut. 1999, 104, 0-205.

Grandjean, P. Developmental fluoride neurotoxicity: An updated review. Environ Health. 2019, 18, 110.

Gareau M. G.; Wine, E.; Rodrigues, D. M.; Cho, J. H.; Whary, M. T.; Philpott, D. J.; Macqueen, G.; Sherman, P. M. Bacterial infection causes stress-induced memory dysfunction in mice. Gut. 2011, 60, 307-17.

Grandjean, P.; Landrigan, P. J. Neurobehavioural effects of developmental toxicity. Lancet Neurol. 2014, 13, 330-8.

Green, R., Lanphear, B., Hornung, R., Flora, D., Martinez-Mier, A., Neufeld, R., Ayotte, P.,Muckle, G., Till, C. Fluoride exposure during fetal development and intellectual abilities in a Canadian birth cohort. Environ Int. 2020, 134, 105315.

Guo, H.; Kuang P.; Luo, Q.; Cui, H.; Deng, H.; Liu, H.; Lu, Y.; Fang, J.; Zuo, Z.; Deng, J.; Li, Y.; Wang, X.; Zhao, L. Effects of sodium fluoride on blood cellular and humoral immunity in mice. Oncotarget. 2017, 8, 85504-85515.

Harry, G. J.; Bruccoleri, A.; d'Hellencourt C. L. Differential modulation of hippocampal chemical-induced injury response by ebselen, pentoxifylline, and TNFα-, IL-1α-, and IL-6-neutralizing antibodies. J Neurosci Res. 2003, 73, 526-36.

Jang, S. E.; Lim, S. M.; Jeong, J. J.; Jang, H. M.; Lee, H. J.; Han, M. J.; Kim D. H. Gastrointestinal inflammation by gut microbiota disturbance induces memory impairment in mice. Mucosal Immunol. 2018, 11, 369-379.

Jeong, H.; Mason, S. P.; Barabási, A. L.; Oltvai, Z. N. Lethality and centrality in protein networks. Nature. 2001, 411, 41-2.

Kesler, S.; Janelsins M.; Koovakkattu D.; Palesh O.; Mustian K.; Morrow Gary.; Dhabhar F. S. Reduced hippocampal volume and verbal memory performance associated with interleukin-6 and tumor necrosis factor-alpha levels in chemotherapy-treated breast cancer survivors. Brain Behav Immun. 2013, 30, S109-16.

Kumar, S.; Pattanaik, A. K.; Sharma, S.; Jadhav, S. E.; Dutta, N.; Avneesh Kumar. Probiotic potential of a *Lactobacillus* bacterium of canine Faecal-Origin and its impact on ielect gut health indices and immune response of dogs. Probiotics Antimicrob Proteins. 2017, 9, 262-277.

Liu, Y. J.; Gao, Q.; Wu, C. X.; Guan Z. Z. Alterations of nAChRs and ERK1/2 in the brains of rats with chronic fluorosis and their connections with the decreased capacity of learning and memory. Toxicol Lett. 2010, 192, 324-9.

Luo, Q.; Cui, H.; Peng X.; Fang, J.; Zuo, Z.; Deng, J.; Liu, J.; Deng, Y. Dietary high fluorine alters intestinal microbiota in broiler chickens. Biol Trace Elem Res. 2016, 173, 483-91.

Luk, G. D.; Bayless, T. M.; Baylin, S. B. Diamine oxidase (histaminase). A circulating marker for rat intestinal mucosal maturation and integrity. J Clin Invest. 1980, 66, 66-70.

Mao, J. H.; Kim, Y. M.; Zhou, Y. X.; Hu, D.; Zhong, C.; Chang, H.; Brislawn, C. J.; Fansler, S.; Langley, S.; Wang, Y.; Peisl, B. Y. L.; Celniker, S. E.; Threadgill, D. W.; Wilmes, P.; Orr, G.; Metz, T. O.; Jansson, J. K.; Snijders, A. M. Genetic and metabolic links between the murine microbiome and memory. Microbiome. 2020, 8, 53.

Mujagic, Z.; Vos P.; Boekschoten, M. V.; Govers, C.; Pieters, H. J.; Wit, N. J. W.; Bron, P. A.; Masclee, A. A. M.; Troos, F. J. The effects of *Lactobacillus plantarum* on small intestinal barrier function and mucosal gene transcription; a randomized double-blind placebo controlled trial. Sci Rep. 2017, 7, 40128.

Mizuno, M.; Yamada, K.; Olariu, A.; Nawa, H.; Nabeshima, T. Involvement of brain-derived neurotrophic factor in spatial memory formation and maintenance in a radial arm maze test in rats. J Neurosci. 2000, 20, 7116-21.

Neuendorf, R.; Harding, A.; Stello, N.; Hanes, D.; Wahbeh, H. Depression and anxiety in patients with Inflammatory Bowel Disease: A systematic review. J Psychosom Res. 2016, 87, 70-80.

Niu, R.; Chen, H.; Manthari, Ram Kumar 1, Zilong Sun 1, Jinming Wang 1, Jianhai Zhang 1, Jundong Wang. Effects of fluoride on synapse morphology and myelin damage in mouse hippocampus. Chemosphere. 2018, 194, 628-633.

Nguyen, T.; Mehta, N. R.; Conant, K.; Kim, K. J.; Jones, M.; Calabresi, P. A.; Melli, G.; Hoke, A.; Schnaar, R. L.; Ming, G. L.; Song, H.; Keswani, S. C.; Griffin, J. W. Axonal protective effects of the myelin-associated glycoprotein. J Neurosci. 2009, 29, 630-7.

Pang, P.T.; Lu, B. Regulation of late-phase LTP and long-term memory in normal and aging hippocampus: role of secreted proteins tPA and BDNF. Ageing Res Rev. 2004, 3, 407-30.

Petrone, P.; Guarinob, F. M.; Giustino, S.; Gombos, F. Ancient and recent evidence of endemic fluorosis in the Naples Area. J Geochem Explor. 2013, 131, 14-27.

Qian, W.; Miao, K.; Li, T.; Zhang, Z. Effect of selenium on fluoride-induced changes in synaptic plasticity in rat hippocampus. Biol Trace Elem Res. 2013, 155, 253-60.

Rafique, T.; Naseem, S.; Ozsvath, D., Hussain, R.; Bhanger, M. I.; Usmani, T. H. Geochemical controls of high fluoride groundwater in Umarkot Sub-District, Thar Desert, Pakistan. Sci Total Environ. 2015, 530-531, 271-278.

Rognes, T.; Flouri, T.; Nichols, B.; Quince, C.; Mahé, F. VSEARCH: a versatile open source tool for metagenomics. PeerJ. 2016, 4, e2584.

Salehipour, Z.; Haghmorad, D.; Sankian, M.; Rastin, M.; Nosratabadi, R.; Dallal, M. M. S.; Tabasi, N.; Khazaee, M.; Nasiraii, L. R.; Mahmoudi, M. Bifidobacterium animalis in combination with human origin of *Lactobacillus plantarum* ameliorate neuroinflammation in experimental model of multiple sclerosis by altering CD4+ T cell subset balance. Biomed Pharmacother. 2017, 95, 1535-1548.

Salucci, S.; Ambrogini, P.; Lattanzi, D,; Betti, M.; Gobbi, P.; Galati, C.; Galli, F.; Cuppini, R.; Minelli A. Maternal dietary loads of alpha-tocopherol increase synapse density and glial synaptic coverage in the hippocampus of adult offspring. Eur J Histochem. 2014, 58, 2355.

Srivastava, S.; Flora, S. J. S. Fluoride in drinking water and skeletal fluorosis: a review of the global impact. Curr Environ Health Rep. 2020, 7, 140-146.

Strandwitz, P. Neurotransmitter modulation by the gut microbiota. Brain Res. 2018, 1693, 128-133.

Sun M. F.; Zhu Y. L.; Zhou Z. L.; Jia X. B.; Xu Y. D.; Yang Q.; Cui C.; Shen Y. Q. Neuroprotective effects of fecal microbiota transplantation on MPTP-induced Parkinson's disease mice: Gut microbiota, glial reaction and TLRLI/TNF-alpha signaling pathway. Brain Behav Immun. 2018, 70, 48-60.

Wang, H.; Sun, Y.; Xin, J.; Zhang, T.; Bai, Y. *Lactobacillus johnsonii* BS15 Prevents psychological stress–induced memory dysfunction in mice by modulating the gut–brain axis. Probiotics Antimicrob Proteins. 2020, doi: 10.1007/s12602-020-09644-9. (Online ahead of print)

Walker, F. R.; Knott, B.; Hodgson, D. M. Neonatal endotoxin exposure modifies the acoustic startle response and circulating levels of corticosterone in the adult rat but only following acute stress. J Psychiatr Res. 2008, 42, 1094-103.

Wei, Y.; Melas, P. A.; Wegener, G.; Mathé, A. A.; Lavebratt, C. Antidepressant-like effect of sodium butyrate is associated with an increase in TET1 and in 5-Hydroxymethylation levels in the Bdnf Gene. Int J Neuropsychopharmacol. 2014, 18, pyu032.

Xin, J.; Zeng, D.; Wang, H.; Ni, X.; Yi, D. Kangcheng Pan, Bo Jing. Preventing non-alcoholic fatty liver disease through *Lactobacillus johnsonii* BS15 by attenuating inflammation and mitochondrial injury and improving gut environment in obese mice. Appl Microbiol Biotechnol. 2014, 98, 6817-29.

Yan, X.; Dong, N.; Hao, X.; Xing Y.; Tian, X.; Feng, J.; Xie, J.; Lv, Y.; Wei, C.; Gao, Y.; Qiu, Y.; Wang, T. Comparative transcriptomics reveals the role of the toll-like receptor signaling pathway in fluoride-induced cardiotoxicity. J Agr Food Chem. 2019, 67, 5033-5042.

Yan, N.; Liu, Y.; Liu, S.; Cao, S.; Wang, F.; Wang, Z.; Xi, S. Fluoride-induced neuron apoptosis and expressions of inflammatory factors by activating microglia in rat brain. Mol Neurobiol. 2016, 53, 4449-60.

Zhao, B.; Wu, J.; Li, J.; Bai, Y.; Luo, Y.; Ji, B.; Xia, B.; Liu, Z.; Tan, X.; Lv, J.; Liu X. Lycopene alleviates DSS-induced colitis and behavioral disorders via mediating microbes-gut-brain axis balance. J Agric Food Chem. 2020, 68, 3963-3975.

Zhan, X.; Stamova, B.; Jin, L. W.; DeCarli, C.; Phinney, B.; Sharp, F. R. Gram-negative bacterial molecules associate with Alzheimer disease pathology. Neurology. 2016, 87, 2324-2332.

Figures

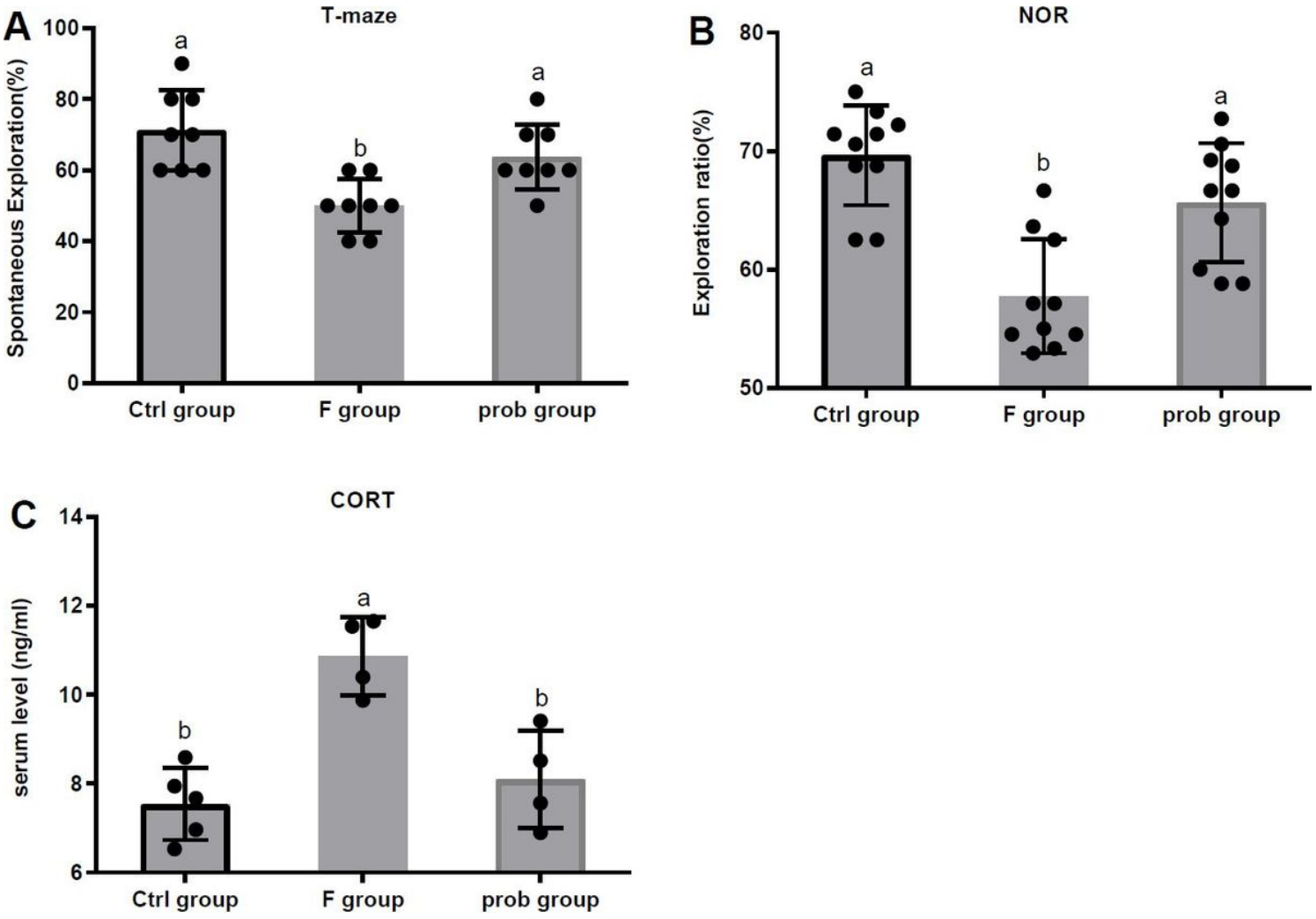

Figure 1

Results of behavioral tests and the serum CORT level. (A) T-Maze, (B) NOR preference tests, and (C) the serum CORT level. Date are presented as the means ± standard deviation. Bars with different letters indicate significant difference on the basis of Duncan's multiple range test ($P<0.05$).

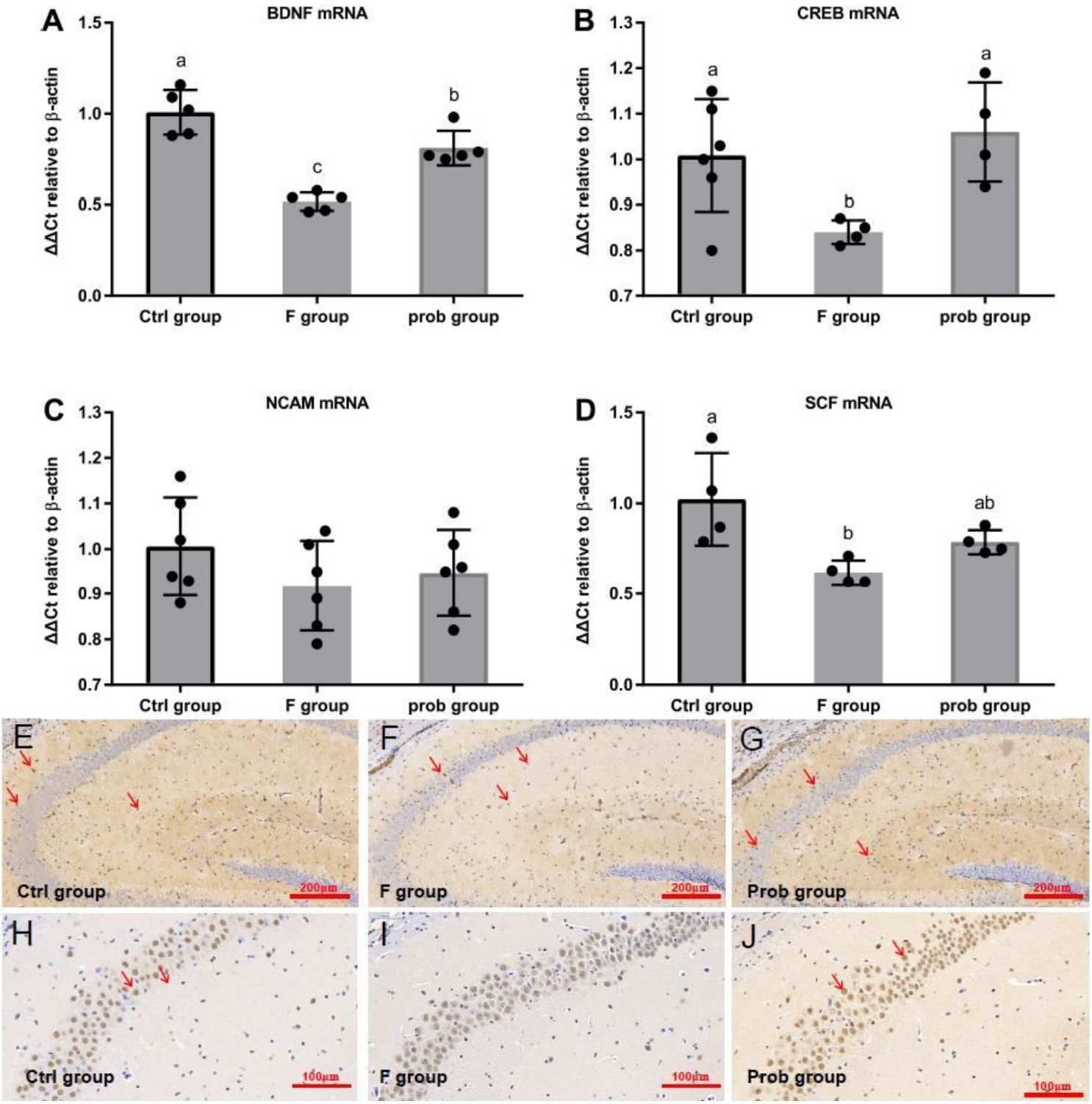

Figure 2

Expressions of neurogenesis-related factors in the hippocampus. Relative expression levels of (A) BDNF, (B) CREB, (C) NCAM, and (D) SCF. Immunohistochemistry of BDNF (E-G) and CREB (H-J) expression in the hippocampus of mice. The BDNF- and CREB-positive cells are brown like the arrow indication. Date are presented as the means ± standard deviation. Bars with different letters indicate significant difference on the basis of Duncan's multiple range test ($P<0.05$).

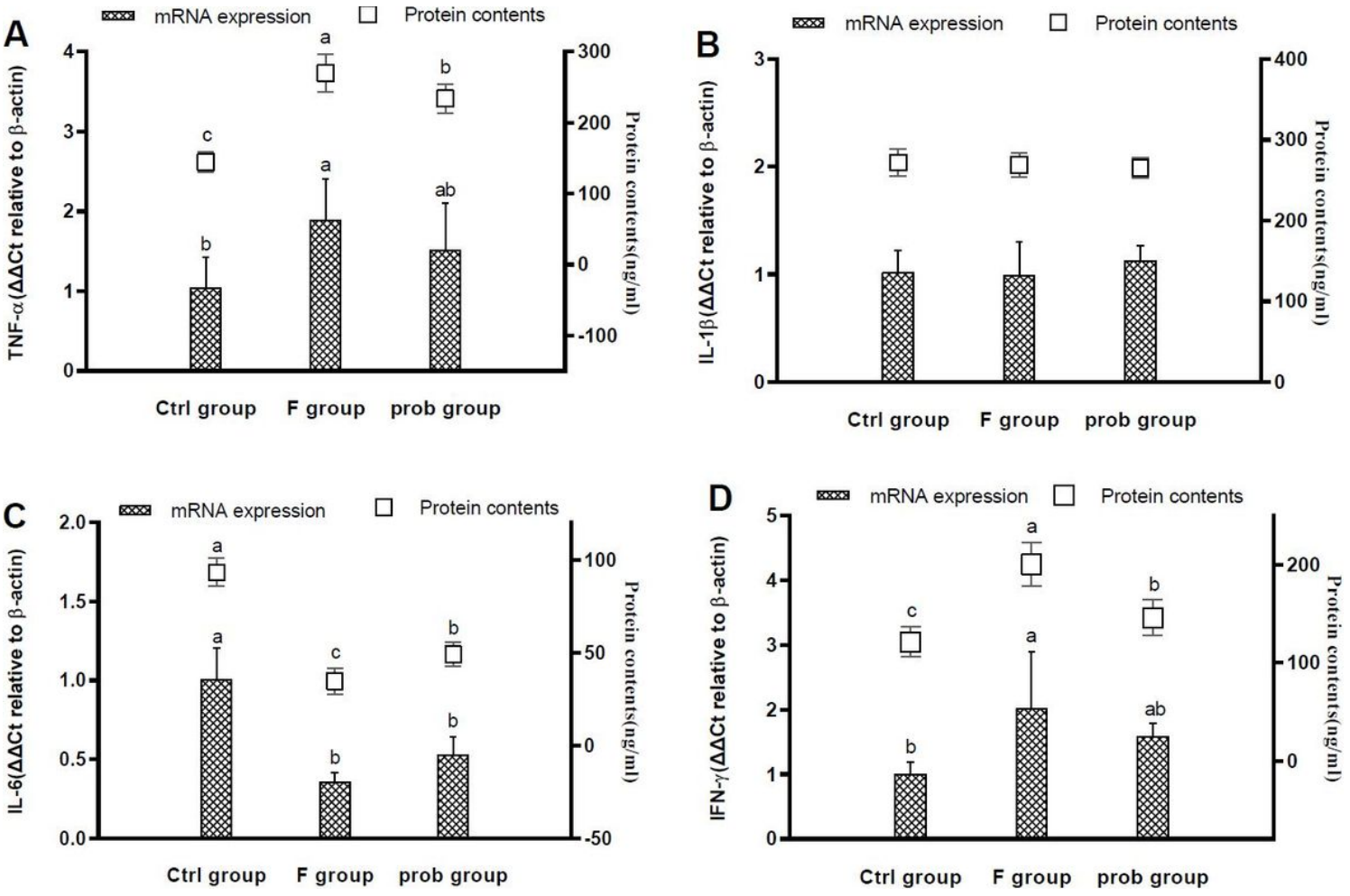

Figure 3

mRNA and protein expression levels of inflammatory cytokines in the hippocampus. Relative expression levels of (A) TNF-α, (B) IL-β, (C) IL-6, and (D) IFN-γ. Data are presented as mean ± standard deviation (n=4–6). Bars with different letters indicate significant difference on the basis of Duncan's multiple range test ($P<0.05$).

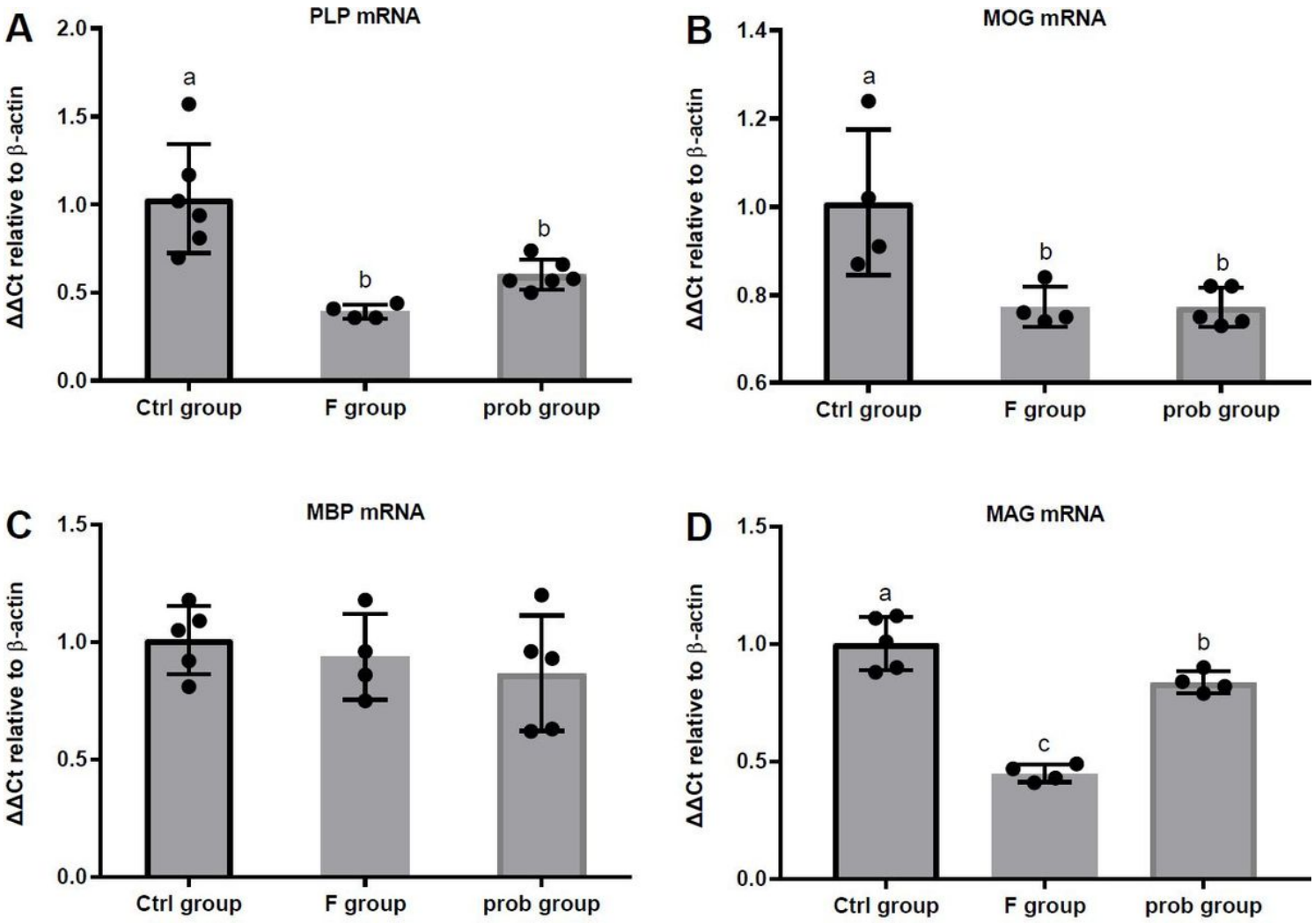

Figure 4

mRNA expression levels of myelin-associated proteins in the hippocampus. Relative expression levels of (A) PLP, (B) MOG, (C) MBP, and (D) MAG. Data are presented as mean ± standard deviation. Bars with different letters indicate significant difference on the basis of Duncan's multiple range test ($p<0.05$).

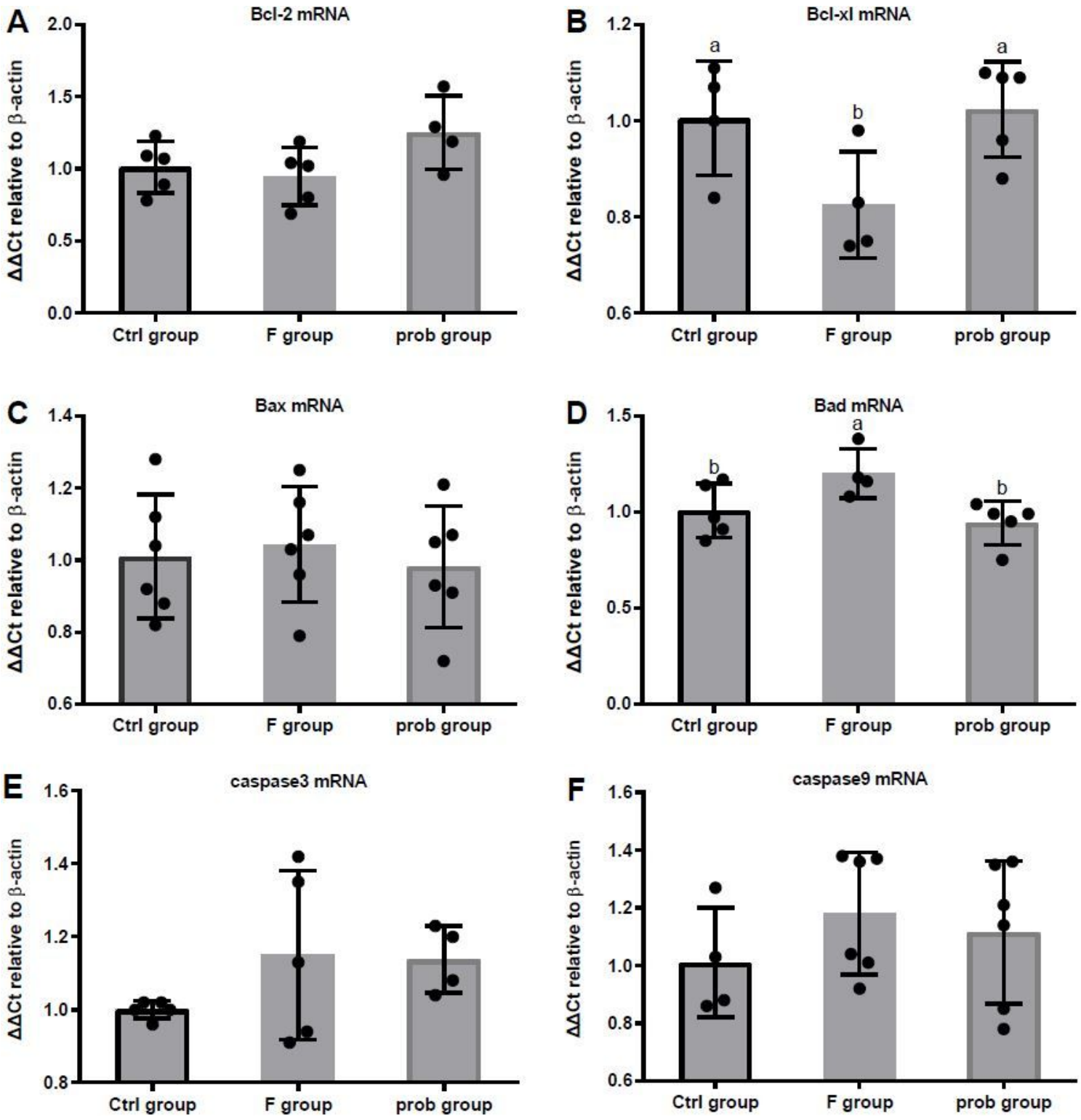

Figure 5

mRNA expression levels of apoptosis-associated proteins in the hippocampus of mice. Relative expression levels of (A) Bcl-2, (B) Bcl-xl, (C) Bax, (D) Bad, (E) caspase-3, and (F) caspase-9. Bars with different letters indicate significant difference ($p<0.05$) on the basis of one-way ANOVA. Each bar represents mean ± standard deviation.

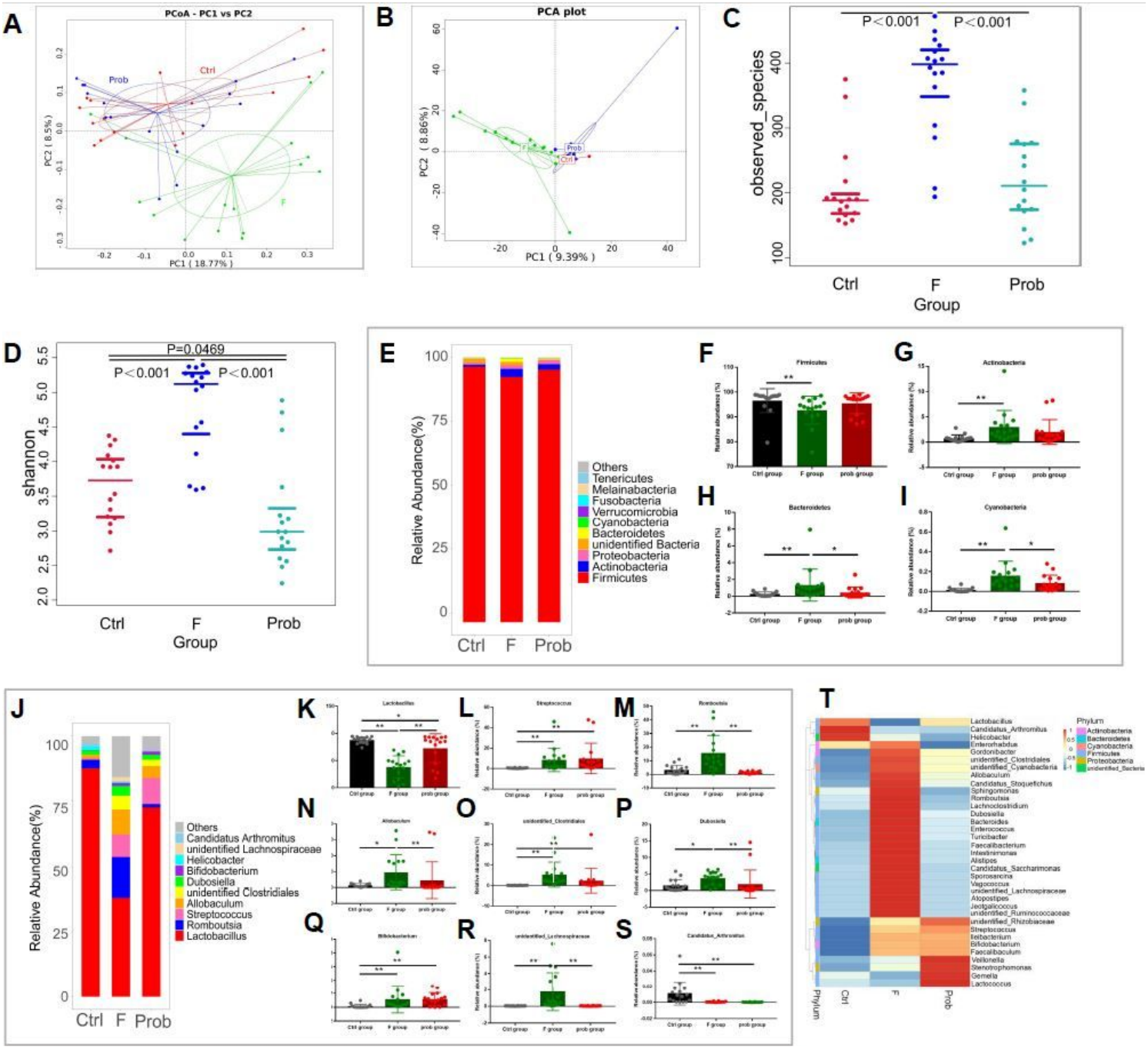

Figure 6

Effects of L. johnsonii BS15 on the gut microbiome structure in fluoride-treated mice. (A) Principal coordinate analysis (PCoA) of unweighted UniFrac distances among the groups. (B) Principal component analysis (PCA) among the groups. (C) Gut microbiome richness (observed species) in ileal luminal samples of each group. Significance: One-way ANOVA and Wilcox. (D) Gut microbiome community diversity (Shannon) in each group. Significance: One-way ANOVA and Wilcox. (E) Relative abundance (%) at the phylum level of each group. (F–I) The relative abundance of gut microbiome with significant difference among the groups in the phylum level. (J) Relative abundance (%) at the genus level of each group. (K–S) The relative abundance of gut microbiome with significant difference among the groups in

the genus level. (T) Genera that are markedly altered by excess fluoride intake compared with the control group and reverted by L. johnsonii BS15. *p < 0.05, **p < 0.01.

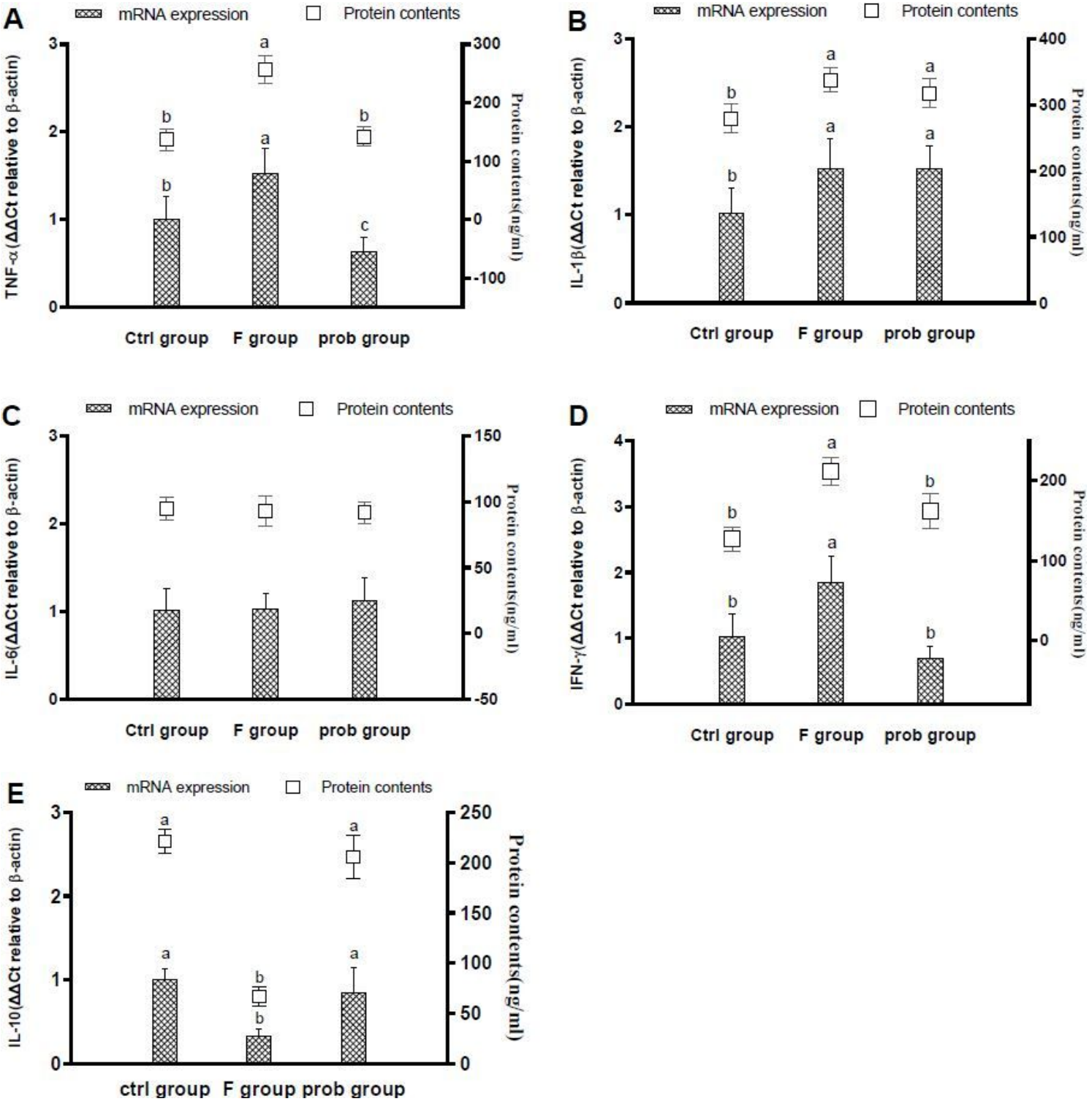

Figure 7

mRNA and protein expression levels of inflammatory cytokines in the ileum. Date are presented as mean ± standard deviation (n=4–6). Bars with different letters indicate significant difference on the basis of Duncan's multiple range test (p<0.05). A-E: Relative expression of TNF-α, IL-β,IL-6, IFN-γ, and IL-10.

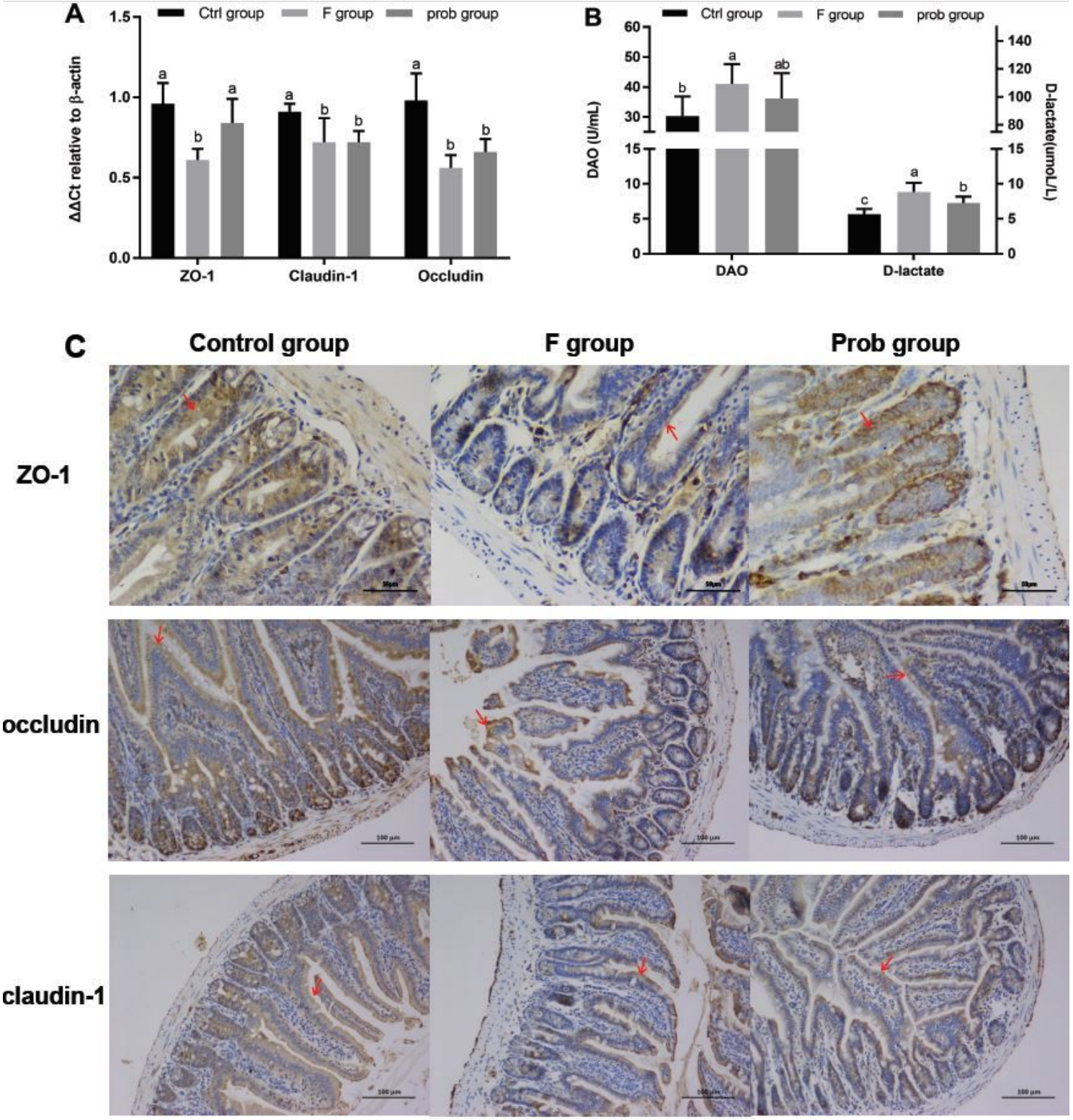

Figure 8

Results of intestinal permeability. (A) mRNA expression levels of ZO-1, claudin-1 and occludin in the ileum, (B) Serum DAO activity and D-lactate concentration. (C) Immunohistochemistry of TJs protein expressions in ileum of mice. The ZO-1-, claudin-1- and occludin-positive cells are brown like the arrow indication. Date are presented as mean ± standard deviation (n=4–6). Bars with different letters indicate significant difference on the basis of Duncan's multiple range test ($p<0.05$).

Supplementary Files

This is a list of supplementary files associated with this preprint. Click to download.

- Additionalfile9.xlsx
- Additionalfile8.pdf
- Additionalfile7.pdf
- Additionalfile6.docx
- Additionalfile5.docx
- Additionalfile4.docx
- Additionalfile3.docx
- Additionalfile2.docx
- Additionalfile1.docx